

High energy pseudogap and its evolution with doping in Fe-based superconductors as revealed by optical spectroscopy

N. L. Wang, W. Z. Hu,* Z. G. Chen, R. H. Yuan, G. Li,† G. F. Chen,‡ and T. Xiang
*Beijing National Laboratory for Condensed Matter Physics,
 Institute of Physics, Chinese Academy of Sciences, Beijing 100190, China*

We report optical spectroscopic measurements on electron- and hole-doped BaFe₂As₂. We show that the compounds in the normal state are not simple metals. The optical conductivity spectra contain, in addition to the free carrier response at low frequency, a temperature-dependent gap-like suppression at rather high energy scale near 0.6 eV. This suppression evolves with the As-Fe-As bond angle induced by electron- or hole-doping. Furthermore, the feature becomes much weaker in the Fe-chalcogenide compounds. We elaborate that the feature is caused by the strong Hund's rule coupling effect between the itinerant electrons and localized electron moment arising from the multiple Fe 3d orbitals. Our experiments demonstrate the coexistence of itinerant and localized electrons in iron-based compounds, which would then lead to a more comprehensive picture about the metallic magnetism in the materials.

PACS numbers: 74.25.Gz, 74.25.Jb, 74.70.-b

I. INTRODUCTION

The interplay between superconductivity and magnetism is one of the central topics in the study of Fe-based superconductors. Similar to the high- T_c cuprates, the superconductivity in Fe-based compounds is found to be in close proximity to an antiferromagnetic (AFM) order^{1,2}. Superconductivity emerges when the magnetic order was suppressed by electron or hole doping or application of pressure^{1,3-5}. Although the phase diagram of Fe-pnictides looks very similar to that of high- T_c cuprates, distinct differences exist between them. The undoped compounds in cuprates are Mott insulators, by contrast, the parent compounds in Fe-pnictides/chalcogenides are multiband metals. Magnetic interaction effect also manifests in the paramagnetic phase. The uniform magnetic susceptibility χ in both parent compounds above T_N and superconducting compounds above T_c is neither Pauli- nor Curie-Weiss-like, instead it increases linearly with increasing temperature within measured temperature range.⁶ Furthermore, the value of χ is roughly two orders larger than the value for a Pauli paramagnetism. Much debates have been focused on whether the magnetism has an itinerant electron or local moment interaction origin, an issue being intimately related to the pairing interaction for superconductivity.

The complex magnetic properties arise from the multiple orbital nature of the systems. The electronic structures of the multiple orbital systems should be also reflected in the charge excitation spectra which could be probed by the optical spectroscopy technique. Previous optical investigations on the parent compounds of AFe₂As₂ (A=Ba, Sr)⁷ revealed clearly the formation of the partial energy gaps at low energy in the magnetic phase, indicating the involvement of the itinerant electrons in the spin-density-wave (SDW) order formation. Nevertheless, the gap opening at low energy is not the sole spectral feature observed with decreasing temper-

ature. As indicated in the early studies,⁷ there exists another remarkable temperature-dependent spectral feature at much higher energy scale. The spectral weight below $\sim 5000 \text{ cm}^{-1}$ (0.6 eV) is gradually suppressed with decreasing temperature and transferred to higher energy scale (see the grey region in Fig. 1). This suppression is observed even at room temperature. This pseudogap-like behavior at such high energy scale is not expected for an usual metal. Although most of the spectral weight at such high energy scale comes from the interband transitions, the temperature dependent part must have a different origin. It has been a long-standing mystery for the Fe-based compounds ever since the optical spectra were collected⁷.

In this work, we address this issue by examining the evolution of the high-energy pseudogap with electron- and hole-dopings. We found that the feature remains strong in the electron-doped side, including in the heavily electron-doped case where the compound is no longer superconducting, but it becomes much weaker in the heavily hole doped case. Our analysis indicates that this high energy gap-like feature is closely related to the doping-induced crystal structural change, particularly the As-Fe-As bond angle, or the height of As position relative to the Fe layers. We elaborate that the high-energy feature is caused by the strong intra-atomic Hund's rule coupling effect due to the presence of multiple Fe 3d orbitals. Our study supports the coexistence of itinerant and localized electrons in iron-pnictides, which would then lead to a more comprehensive picture about the metallic magnetism in the materials.

II. EXPERIMENT

Single crystals of K- and Co-doped BaFe₂As₂ were grown from the FeAs flux method, similar to the procedure in our earlier report.⁸ The plate-like crystals could be easily cleaved, resulting in very shiny sur-

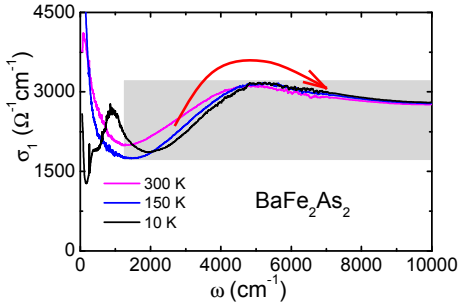


FIG. 1: (Color online) Optical conductivity spectra up to 10000 cm^{-1} (~ 1.2 eV) for a BaFe_2As_2 single crystal.⁷

face. We present four different samples: two K-doped $\text{Ba}_{1-x}\text{K}_x\text{Fe}_2\text{As}_2$ with $x=0.4$ ($T_c=37$ K) and $x=1$ ($T_c=3$ K), and two Co-doped $\text{BaFe}_{2-y}\text{Co}_y\text{As}_2$ with $y=0.2$ ($T_c=22$ K) and $y=0.4$ (not superconducting). We also compare the measurement data with the parent compounds BaFe_2As_2 and $\text{Fe}_{1.05}\text{Te}$. It is well known that the K^+ doping for Ba^{2+} introduces extra holes. On the other hand, NMR experiment indicated that Co^{2+} doping for Fe^{2+} does not induce local moment but offer one more d-electron to the system, therefore has the effect of electron-doping.⁹ Roughly, $T_c=37$ K and 22 K are close to the highest superconducting transition temperatures achieved by K-doping (off FeAs plane) and Co-doping (within FeAs plane), respectively, *i.e.* they are optimally doped. However, $\text{BaFe}_{1.6}\text{Co}_{0.4}\text{As}_2$ is heavily electron-doped, and KFe_2As_2 is heavily hole-doped. The phase diagram of the K- and Co-doped BaFe_2As_2 is shown in Fig. 2.^{10,11} The studied compositions are indicated in the figure.

The optical reflectance measurements were performed on a combination of Bruker IFS 66v/s, 113v on newly cleaved surfaces (ab-plane) of those crystals up to 25000 cm^{-1} . An *in situ* gold and aluminium overcoating technique was used to get the reflectivity $R(\omega)$. The real part of conductivity $\sigma_1(\omega)$ is obtained by the Kramers-Kronig transformation of $R(\omega)$.

III. RESULTS AND DISCUSSIONS

Figure 3 show the experimental reflectance and conductivity spectra for different samples. For a comparison, we also include the data of BaFe_2As_2 ⁷ and $\text{Fe}_{1.05}\text{Te}$ ¹² compounds. The low frequency data vary significantly for those samples because of the different ground states. Superconducting pairing energy gap features exist in the Co-doped (Co=0.2) and K-doped (K=0.4) superconducting samples at very low frequencies (not visible clearly in the plot over such broad energy scale). Clear SDW gap features were seen for the pure BaFe_2As_2 sample. Purely metallic temperature-dependent responses were observed for the heavily electron- or hole-doped samples. But here we focus our attention on the high energy gap-like spec-

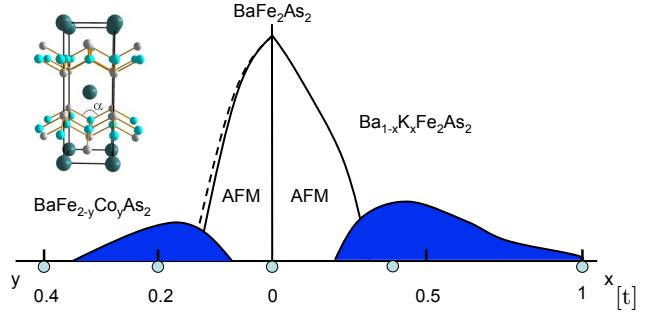


FIG. 2: (Color online) Phase diagram of Co- and K-doped BaFe_2As_2 .^{10,11} Optical data were presented on five different compositions as indicated in the bottom of the phase diagram. The crystal structure of 122 compound is shown. The As-Fe-As angle is indicated by the angle α .

tral weight suppression features.

In optical reflectance spectrum $R(\omega)$, the high energy structure manifests itself as a suppression of $R(\omega)$ in the mid-infrared region (about 2000-5000 cm^{-1}). As the low- ω $R(\omega)$ still increases towards unit due to metallic nature of the compounds, a reverse S-like shape in $R(\omega)$ is resulted. In Fig. 3 we find that, compared to the parent BaFe_2As_2 compounds, the reverse S-like shape $R(\omega)$ remains rather eminent in the Co-doped compounds. However, the feature becomes weaker in K=0.4 doped case, and tends to disappear in the pure KFe_2As_2 sample with T_c only 3 K. The feature is also not visible in $\text{Fe}_{1.05}\text{Te}$.

Corresponding to the reverse S-like shape of $R(\omega)$, the real part of conductivity $\sigma_1(\omega)$ shows a suppression roughly below 5000 cm^{-1} . This leads to a peak in $\sigma_1(\omega)$ near this energy, as shown in Fig. 3. Our earlier study on the parent compound indicated that the suppressed spectral weight is transferred to higher energies,⁷ indicating a pseudogap-like phenomenon.

To further elaborate the spectral evolution, we plot the frequency-dependent spectral weight of $\sigma_1(\omega)$ at 10 and 300 K for two different crystals, the parent BaFe_2As_2 and Co-doped $\text{BaFe}_{1.6}\text{Co}_{0.2}\text{As}_2$, in Fig. 4. For the parent BaFe_2As_2 , a residual Drude component exists in the SDW state.⁷ This residual Drude component narrows with decreasing temperature, and its low-frequency limit approaches the dc conductivity value. As a result, the low- ω spectral weight, roughly below 200 cm^{-1} , at low T is higher than at high T. Above 200 cm^{-1} , the SDW gap develops which strongly reduces the low-T Drude weight, leading to the first suppression below 1000 cm^{-1} . The lost Drude weight fills into the SDW peak, and the total spectral weight is almost recovered around 2000 cm^{-1} for 10 K. However, the T-dependent suppression below the mid-infrared peak results in the second spectral weight suppression at 10 K near 3000 cm^{-1} . The lost weight gradually recovers at very high energy, roughly about 10000 cm^{-1} . For the Co-doped $x=0.2$ crystal, there is no SDW gap developing at low temperature, the low- ω spectral weight change is induced by the Drude component narrowing. A balance is seen near 1200 cm^{-1} . The

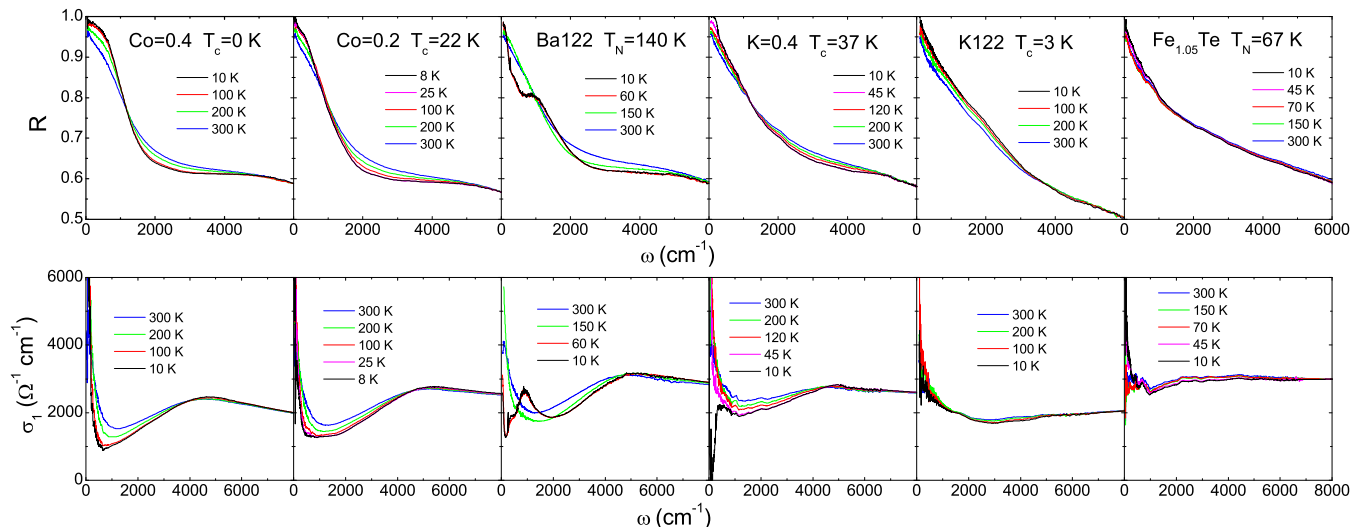


FIG. 3: (Color online) The evolution of the optical spectra of BaFe_2As_2 with Co- and K-doping. $\text{Fe}_{1.05}\text{Te}$ is added for comparison. Upper panel: $R(\omega)$ for the pure, Co- and K-doped BaFe_2As_2 and $\text{Fe}_{1.05}\text{Te}$ up to 6000 cm^{-1} . Lower panel: $\sigma_1(\omega)$ for the pure, Co- and K-doped BaFe_2As_2 and $\text{Fe}_{1.05}\text{Te}$ up to 8000 cm^{-1} .

further reduction of the spectral weight beyond this frequency at low temperature is caused by the gap-like suppression near 5000 cm^{-1} . Once again, the recovery of the spectral weight extends to rather high energy scale. We should remark that, at such high energy scale, most of the spectral weight would come from the interband transitions. However, the temperature-dependent part must have a different origin. Seen clearly from Fig. 3, the pseudogap feature remains very strong for all Co-doped superconducting samples, but become weak in the K-doped compounds and tends to vanish for the pure KFe_2As_2 . No suppression feature is visible in $\sigma_1(\omega)$ for $\text{Fe}_{1.05}\text{Te}$.

The key issue here is the origin of this high energy pseudogap. Unlike the spin-density-wave gap observed for the parent compounds only below magnetic ordering temperature, the high energy pseudogap feature is present at all measurement temperatures as well as in the doped compounds, as indicated in Fig. 3. There could be several possibilities for the presence of high energy peak structure. One possibility is that the quasi-particles con-

tain not only the coherent spectral weight at low energy but also the incoherent part at high energies due to the presence of strong electron correlation effect.^{13–15} The high energy feature comes from the incoherent part of the quasi-particle spectral function. This should be a generic phenomenon for strongly correlated electron system. A schematic picture about the quasi-particle spectral weight function is shown in Fig. 5. The incoherent part is argued to originate from the onset Hubbard U . A dynamical mean-field theory calculation indicated that both the incoherent structures at intermediate frequencies of the order $U/2$ to U and the coherent Drude component at the lower end of the conductivity spectrum rapidly emerge as the temperature is lowered.^{13,14} This has been used to explain the experimental observation of development of both Drude component and mid-infrared peak at low temperature in V_2O_3 .¹⁴ However, this is different from the present case where the Drude component already exists in Fe-based compounds at high temperatures. Furthermore, this picture is rather difficult to explain the doping evolution of the structure. In particular, $\text{Fe}_{1.05}\text{Te}$ is believed to have stronger electron correlation, but the temperature-dependent feature at mid-infrared is almost invisible. In fact, the conductivity spectrum in the mid-infrared region even has slightly lower values at lower temperature.

A different but related proposal is that the coherent spectrum at low frequency is due to the itinerant electrons from some Fe 3d orbitals which form the disconnected electron and hole Fermi surfaces, while the incoherent part is due to the Hubbard U splitting of the localized bands from other Fe 3d orbitals.^{16,17} The occupation of the electrons at the lower Hubbard band results in the formation of local moments. In our opinion, this scenario also faces great challenges. The electron correlations in Fe-based compounds are not so strong. The

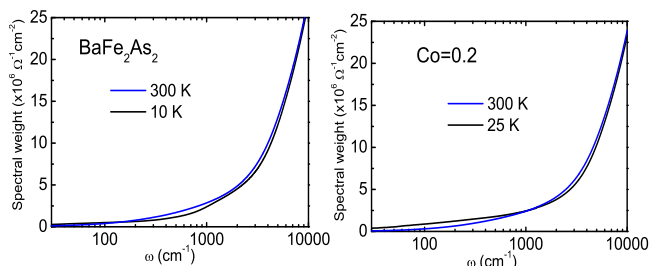


FIG. 4: (Color online) The integrated spectral weight below 10000 cm^{-1} for BaFe_2As_2 and $\text{BaFe}_{1.6}\text{Co}_{0.2}\text{As}_2$ single crystals.⁷

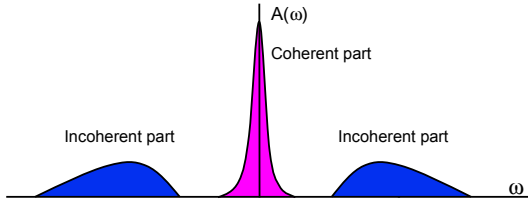


FIG. 5: (Color online) The spectral function of a correlated electron system. It contains both coherent part at low frequency and incoherent part at higher frequencies. The incoherent part could lead to sizeable spectral weight at mid-infrared region.

band renormalization factors were found to be only about 2-3.¹⁸⁻²¹ Furthermore, some orbitals are almost degenerate. It is hard to image that those bands could be split by the relatively weak on-site electron correlation.

Because the feature is temperature dependent, one may think that it is related to the spin-fluctuations. A naive idea is that the feature is caused by the indirect interband transitions assisted by the spin fluctuations with an AFM (π, π) wave vector. As shown schematically in Fig. 6, the hole and electron bands are well connected by such commensurate wave vector $\mathbf{q}=(\pi, \pi)$ in the BaFe_2As_2 parent compound. The indirect interband transition could be realized through the assistance of (π, π) spin fluctuations with the transition energy of $h\nu=E_f-E_i+\Omega$, where E_i and E_f are the energy levels of the initial and final states of the particle hole excitations, Ω is the energy corresponding to the formation of fluctuated AFM correlation which usually have a rather small energy scale. However, a careful examination indicates that this possibility is also unlikely. First, the bands close to the Γ and M points are better connected by the (π, π) wave vector, the lower energy region is expected to have higher indirect interband transition spectral weight with decreasing temperature, which is opposite to the suppression spectral feature at lower frequencies. Second, the opposite trend between electron- and hole-dopings highly suggests against this scenario. The (π, π) spin-fluctuations are believed to be strongly suppressed in either heavily electron- or hole-doped compounds. Then, it is difficult to understand why they change in the opposite ways.

We propose that the high energy feature reflects the presence of local physics. The spectral weight transfer from low energy to high energy implies a transfer of relatively itinerant electrons with binding energy less than 0.6 eV to the more localized part. A promising picture is as follows. The Fe-pnictides/chalcogenides contain both itinerant electrons and local moments arising from different 3d orbitals of the iron atoms. Unlike the proposals mentioned above, the local moment formation is not caused by the Hubbard U interaction but mainly originate from the Hund's rule coupling interaction of the different orbitals. If the Hund's rule coupling energy is smaller than the kinetic energy (or band width) of elec-

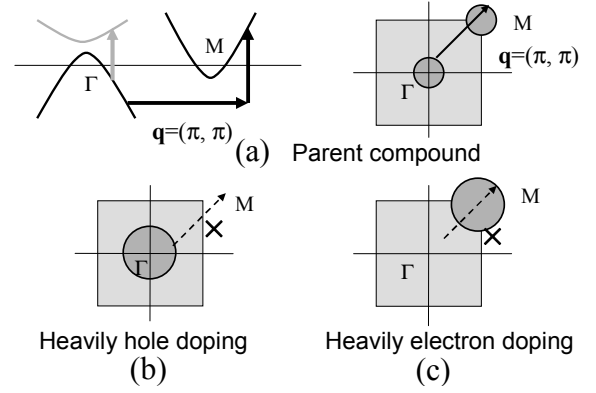


FIG. 6: A schematic picture for the band structure evolution. For the parent BaFe_2As_2 , indirect interband transitions between the hole and electron bands could occur with the help of the $\mathbf{q}=(\pi, \pi)$ AF spin fluctuations. For the heavily hole-doped compound, e.g. pure KFe_2As_2 , the chemical potential shifts downward, which leads to the removal of the electron FS near M point and associated AF correlation (b). For the heavily electron (Co-) doped case, the chemical potential shifts up, leading to the removal of the hole FS surface near Γ (c). In both cases, (π, π) AF fluctuations are strongly suppressed. The spin fluctuation-assisted indirect interband transition should be significantly reduced.

trons in some orbitals, those electrons are itinerant. On the other hand, if the Hund's coupling energy is larger than the kinetic energy of the electrons in other orbitals, those electrons are localized and form local moments. In general, the itinerant electrons and local moments are not completely isolated, but are also coupled via the Hund's rule interaction, as illustrated in Fig. 7. We identify the energy scale of the suppression near 0.6 eV as the local Hund's rule coupling energy scale. This value is indeed close to those estimated in a number of the theoretical works²²⁻²⁶ and a resonant inelastic x-ray scattering (RIXS) experiment²⁷. At low temperature, the thermal excitations become weak, then a fraction of relatively itinerant electrons tend to become more localized. Thus, we would expect to observe the spectral weight transfer from low energy to an energy scale higher than the Hund's rule coupling energy.

The above picture provides a natural explanation for the experimental observation in the optical measurement. Nevertheless, there are two crucial questions which have to be addressed. First, why a relatively small change of temperature from 300 K to 10 K could lead to such an apparent spectral weight transfer over very broad frequency range, that is, from far below 0.6 eV to far above it? Second, why the spectral weight transfer feature evolves significantly with electron or hole doping?

To understand the first question, we have to assume that the kinetic energies of the electrons in different Fe 3d bands/orbitals are relatively close. Some may be slightly larger than the Hund's rule coupling energy, while others may be slightly smaller than the Hund's rule coupling

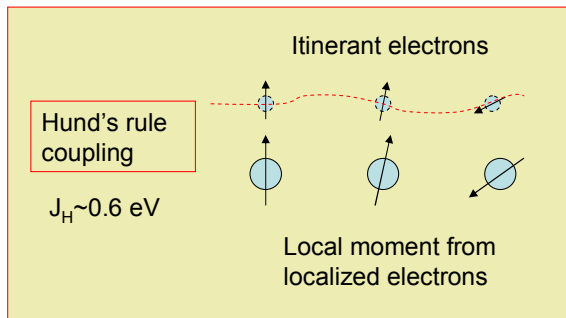


FIG. 7: A schematic picture about the Hund's coupling between itinerant electrons and local moments. The local moment tends to polarize the spin of the itinerant electrons in a ferromagnetic orientation. At low T, itinerant electrons tends to become more localized due to this coupling, leading to the spectral weight transfer from low energy to higher energies.

energy. In other words, the energy levels or bands that contribute to the local moments are rather close to the Fermi level where itinerant electrons dominate, so that the temperature change could affect their interaction. Indeed, the first principle band structure calculations on LaFeAsO and Ba122 indicated that all 5 orbitals of Fe 3d electrons are rather close in energy.²¹ The local moments estimated from the density function calculations are usually higher than $2\mu_B$, suggesting more than 2 electrons are localized which contribute to the local moments. The situation is somewhat similar to the element α -Fe, which has been known for several decades for the presence of both itinerant and localized d electrons. It deserves to remark that the recent neutron^{28,29} and RIXS experiments revealed presence of large local moments in both parent compounds above T_N and doped superconducting compounds above T_c .

An important observation in the present work is that the spectral weight transfer feature changes with doping, particularly in the K-doped case. From the crystal structural characterization, it is found that the K-doping results in a continuous decrease of the a-axis but an increase of the c-axis parameters. More detailed analysis indicates that K-doping does not induce detectable change in the Fe-As bonding length, but lead to a continuous decrease of As-Fe-As angle (the α angle in the crystal structure shown in Fig. 2)¹¹. Equivalently, the height of As atom relative to the Fe-layer is increasing. The As height in FeTe is further increased compared to Fe-pnictides.²² On the contrary, the Co-doping does not lead to an detectable change in the a-axis lattice parameter but only a slight decrease of c-axis parameter³⁰. According to the

band structural calculations, the band structure is rather sensitive to the As height relative to the Fe layer.^{22,24,25} The increase of As height mainly make the Fe atom more isolated, leading to the narrowing the Fe 3d bands. As a result, the effective Hund's rule coupling is enhanced.²² Then the spectral weight suppression feature could not be seen within a temperature range change from 300 to 10 K. Higher temperature range would be required in order to see the spectral weight transfer structure. We found that the picture could well explain the doing evolution and the disappearance of the feature in Fe_{1.05}Te.

Finally, we comment on the spin-density-wave gap formation on the Fe-pnictide compounds. Based on the above study, the local moment formation itself is not due to the Fermi surface nesting, but caused by the strong Hund's rule coupling between different Fe 3d orbitals. However, the Fermi surfaces couple strongly with the magnetic instability. A spin-density-wave gap would open once the nesting of FS's matches with the magnetic wave vector.

IV. SUMMARY

In conclusion, our measurement indicates that the FeAs compounds are not simple itinerant electron systems. The optical data of the 122 parent compound and their evolution with K- and Co-doping revealed spectral change not only at low but also considerable high frequencies. The spectral structure and its evolution implies the presence of both itinerant and localized electrons arising from different Fe 3d orbitals. We elaborate that the spectral weight transfer over the broad energies is related to the Hund's rule coupling between itinerant and localized electrons. The coupling effect could be strongly affected by the environment of Fe atom, i.e. the bonding angle of As-Fe-As or the height of As atom relative to the Fe layer. Our experiments demonstrate the coexistence of itinerant and localized electrons in iron-based compounds, which would then lead to a more comprehensive picture about the metallic magnetism in the materials.

Acknowledgments

We would like to thank Z. Y. Weng, T. Egami, W. Ku, W. G. Yin, H. J. Choi, G. M. Zhang, J. P. Hu, J. L. Luo, D. H. Lee, Z. Fang, X. Dai for helpful discussions. This work is supported by the NSFC, CAS, and the 973 project of the MOST of China.

* Present address: Max Planck Department for Structural Dynamics, University of Hamburg, Centre for Free Electron Laser Science, Notkestraße 85, 22607 Hamburg, Germany

† Present address: National High Magnetic Field Laboratory, Florida State University, Tallahassee, Florida 32310, USA

‡ Present address: Department of Physics, Renmin Univer-

- sity of China, Beijing 100872, China
- ¹ J. Dong, H. J. Zhang, G. Xu, Z. Li, G. Li, W. Z. Hu, D. Wu, G. F. Chen, X. Dai, J. L. Luo, Z. Fang, and N. L. Wang, *Europhys. Lett.* **83**, 27006 (2008).
 - ² Clarina de la Cruz, Q. Huang, J. W. Lynn, Jiying Li, W. Ratcliff II, J. L. Zarestky, H. A. Mook, G. F. Chen, J. L. Luo, N. L. Wang, and Pengcheng Dai, *Nature* **453**, 899 (2008).
 - ³ G. F. Chen, Z. Li, D. Wu, G. Li, W. Z. Hu, J. Dong, P. Zheng, J. L. Luo, and N. L. Wang, *Phys. Rev. Lett.* **100**, 247002 (2008).
 - ⁴ M. Rotter, M. Tegel, D. Johrendt, *Phys. Rev. Lett.* **101**, 107006 (2008).
 - ⁵ M. S. Torikachvili, S. L. Bud'ko, N. Ni, P. C. Canfield, *Phys. Rev. Lett.* **101**, 057006 (2008).
 - ⁶ G. M. Zhang, Y. H. Su, Z. Y. Lu, Z. Y. Weng, D. H. Lee, and T. Xiang, *Europhys. Lett.* **86**, 37006 (2009).
 - ⁷ W. Z. Hu, J. Dong, G. Li, Z. Li, P. Zheng, G. F. Chen, J. L. Luo, and N. L. Wang, *Phys. Rev. Lett.* **101**, 257005 (2008).
 - ⁸ G. F. Chen, Z. Li, J. Dong, G. Li, W. Z. Hu, X. D. Zhang, X. H. Song, P. Zheng, N. L. Wang, J. L. Luo, *Phys. Rev. B* **78**, 224512 (2008).
 - ⁹ F.L. Ning, K. Ahilan, T. Imai, A. S. Sefat, R. Jin, M. A. McGuire, B. C. Sales, and D. Mandrus, *J. Phys. Soc. Jpn.* **77**, 103705 (2008).
 - ¹⁰ J. H. Chu, J. G. Analytis, C. Kucharczyk, and I. R. Fisher, *Phys. Rev. B* **79**, 014506 (2009).
 - ¹¹ M. Rotter, M. Pangerl, M. Tegel, and D. Johrendt, *Angew. Chem. Int. Ed.* **47**, 7949 (2008).
 - ¹² G. F. Chen, Z. G. Chen, J. Dong, W. Z. Hu, G. Li, X. D. Zhang, P. Zheng, J. L. Luo, and N. L. Wang, *Phys. Rev. B* **79**, 140509(R) (2009).
 - ¹³ A. Georges, G. Kotliar, W. Krauth and M. J. Rozenberg, *Rev. Modern. Phys.* **68**, 13 (1996).
 - ¹⁴ M. J. Rozenberg, G. Kotliar, H. Kajueter, G. A. Thomas, D. H. Rapkine, J. M. Honig, and P. Metcalf, *Phys. Rev. Lett.* **75**, 105 (1995).
 - ¹⁵ Qimiao Si, *Nature physics* **5**, 629 (2009).
 - ¹⁶ Su-Peng Kou, Tao Li, and Zheng-Yu Weng, *Europhys. Lett.* **88**, 17010 (2009).
 - ¹⁷ Yi-Zhuang You, Fan Yang, Su-Peng Kou, and Zheng-Yu Weng, arXiv:1102.3200.
 - ¹⁸ M. M. Qazilbash, J. J. Hamlin, R. E. Baumbach, Lijun Zhang, D. J. Singh, M. B. Maple, D. N. Basov, *Nature Physics* **5**, 647 (2009).
 - ¹⁹ Z. G. Chen, R. H. Yuan, T. Dong, N. L. Wang, *Phys. Rev. B* **81**, 100502(R) (2010).
 - ²⁰ M. Yi, D. H. Lu, J. G. Analytis, J.-H. Chu, S.-K. Mo, R.-H. He, X. J. Zhou, G. F. Chen, J. L. Luo, N. L. Wang, Z. Hussain, D. J. Singh, I. R. Fisher, and Z.-X. Shen, *Phys. Rev. B* **80**, 024515 (2009).
 - ²¹ D. J. Singh, *Physica C* **469**, 418 (2009).
 - ²² Wei-Guo Yin, Chi-Cheng Lee, and Wei Ku, *Phys. Rev. Lett.* **105**, 107004 (2010).
 - ²³ K. Haule, J. H. Shim, and G. Kotliar, *Phys. Rev. Lett.* **100**, 226402 (2008).
 - ²⁴ G. T. Wang, Y. M. Qian, G. Xu, X. Dai, Z. Fang, *Phys. Rev. Lett.* **104**, 047002 (2010).
 - ²⁵ Chang-Youn Moon and Hyoung Joon Choi, *Phys. Rev. Lett.* **104**, 057003 (2010).
 - ²⁶ M. D. Johannes, Igor Mazin Journal-ref: *Phys. Rev. B* **79**, 220510R (2009).
 - ²⁷ W. L. Yang, P. O. Velasco, J. D. Denlinger, A. P. Sorini, C.-C. Chen, B. Moritz, W.-S. Lee, F. Vernay, B. Delley, J.-H. Chu, J. G. Analytis, I. R. Fisher, Z. A. Ren, J. Yang, W. Lu, Z. X. Zhao, J. van den Brink, Z. Hussain, Z.-X. Shen, T. P. Devereaux, *Phys. Rev. B* **80**, 014508 (2009)
 - ²⁸ Zhijun Xu, Jinsheng Wen, Guangyong Xu, Songxue Chi, Wei Ku, Genda Gu, and J. M. Tranquada, arXiv:1012.2300.
 - ²⁹ Igor A. Zaliznyak, Zhijun Xu, John M. Tranquada, Genda Gu, Alexei M. Tsvetlik, Matthew B. Stone, arXiv:1103.5073.
 - ³⁰ D.L. Sun, J.Z.Xiao, and C.T.Lin, *Journal of Crystal Growth* **321**, 55 (2011).